Regional Environmental Change (2019) 19:2507–2519
https://doi.org/10.1007/s10113-019-01575-8

ORIGINAL ARTICLE

A spatially explicit reconstruction of cropland based on expansion of polders in the Dongting Plain in China during 1750–1985

Yikai Li[1] · Yu Ye[1,2] · Chengpeng Zhang[1] · Jun Li[1] · Xiuqi Fang[1]

Received: 13 May 2019 / Accepted: 4 October 2019 / Published online: 4 November 2019

Abstract

Global historical cropland datasets allocate cropland areas into grids above on the assumption that land suitable for crops is similar to that in the present or changeless over time. However, land suitability has changed over time. The Dongting Plain, which is full of polders, is characterized by changing land suitability for crops over the past 300 years and provides a case study of the impact of changing land suitability on spatially explicit reconstructions. Here, cropland areas were reconstructed at the county level and allocated into grids at 0.5′ × 0.5′. This allocation was based on the expansion of polders, which indicated land suitable for crops. The results showed the following: (1) The land suitable for crops constituted 68.24% of the total area in 1750 and it expanded after 1850, which in 1911, 1949, and 1985 was 1.10, 1.18, and 1.25 times that of 1750, respectively. (2) The regional cropland area fraction was 21.60% in 1750 and it increased after 1850, which in 1911, 1949, and 1985 was 127.21%, 140.27%, and 156.03% that of 1750. (3) The grids with cropland fractions increased due to polder development by more than 30% in the middle of the region from 1750 to 1985, occupying 32.16% of the total grids. (4) Changes in the land suitability for crops impacted the spatially explicit reconstruction. The grids unsuitable for crops were 78, 46, and 28 in 1850, 1911, and 1949 at 0.5′ × 0.5′, which constituted 19.21%, 11.33%, and 6.90% of the total grids, respectively. In comparison with this study, some of the grids unsuitable for crops were allocated as cropland by HYDE 3.2 and covered 93.59%, 89.13%, and 82.14% of the total unsuitable girds.

Keywords Historical cropland change · Spatially explicit reconstruction · Land suitability for crops · Wetland · Polder · Dongting Plain in Hunan

Introduction

The land cover change induced by land use affects the biodiversity of terrestrial ecosystems and influences the global and regional climate by changing the physical processes of the land surface (e.g., surface albedo and roughness) and the biogeochemical cycles (e.g., carbon, phosphorus, and nitrogen) (Ellis et al. 2013; Bayer et al. 2017; Erb et al. 2017; Gaillard et al. 2018). As the basis for studying the impact of land use/cover change (LUCC) on global change, several global historical cropland datasets, such as HYDE (History Database of the Global Environment), SAGE (Center for Sustainability and the Global Environment), and KK10 (Kaplan and Krumhardt), have been developed, which have been applied in many studies on global change (Ellis et al. 2013; Gaillard et al. 2018). Among the global historical cropland datasets, HYDE is developed by the Netherlands Environmental Assessment Agency (Goldewijk 2001; Goldewijk et al. 2011; Goldewijk et al. 2017), and its latest renewed version (HYDE 3.2) is reconstructed croplands and pastures with a

Communicated by Jasper van Vliet

✉ Yu Ye
yeyuleaffish@bnu.edu.cn

Yikai Li
lyk2016@mail.bnu.edu.cn

Chengpeng Zhang
cpzhang@mail.bnu.edu.cn

Jun Li
lixiaojun@mail.bnu.edu.cn

Xiuqi Fang
xfang@bnu.edu.cn

[1] Faculty of Geographical Science, Beijing Normal University, Beijing 100875, China

[2] Key Laboratory of Environment Change and Natural Disaster, Ministry of Education, BNU, Beijing 100875, China

spatial resolution of 0.5′ × 0.5′ from 10,000 BC to AD 2015 (Goldewijk et al. 2017); SAGE with a spatial resolution of 0.5° × 0.5° and coverage of AD 1700–1992 is developed by the Center for Sustainability and the Global Environment of University of Wisconsin (Ramankutty and Foley 1999); and KK10 is developed by Kaplan and Krumhardt (Kaplan et al. 2009; Kaplan et al. 2011), which shows the change in cropland and deforestation with a spatial resolution of 0.5′ × 0.5′ during 8 ka BP-AD 1850.

For reconstruction of histrical cropland data, the current global historical LUCC datasets are developed by allocating the total historical cropland area of continents or countries into the grids according to reclamation suitability, which is calculated by land suitability models constructed by the selected natural factors having an effect on crop growth and cropland spatial distribution (Kaplan et al. 2009; Goldewijk et al. 2017). According to the order of the reclamation suitability of each spatial unit, the cropland area in the form of cropland fraction is allocated to each grid within the spatial scope of modern cropland (Kaplan et al. 2009; Goldewijk et al. 2017).

The cropland allocation mentioned above was made on the assumption that the land suitability for crops is similar to that in the present or changeless over time. However, land suitability for reclamation changes through time due to environmental change or human activities. For example, in the Lesvos in Greece, the cropland abandoned due to soil erosion that was cultivated in the late nineteenth century has been distributed outside the scope of modern cropland (Bakker et al. 2005); the Alamo valley in the Western United States, which was originally too dry to be suitable for farming, has been reclaimed since the twentieth century because of irrigation technology (Garcia-Acevedo 2001); the croplands in the southwest of Bangladesh's Ganges Delta have increased with a growing number of dikes after the 1960s, where was once lacked cropland because of frequent flooding before the mid-twentieth century (Auerbach et al. 2015). The historically changing land suitability for crops could directly affect the allocation reliability of cropland fractions. Hence, it is necessary to consider changes in land suitability over time when spatially explicit reconstructions of cropland change are carried out in such areas.

Wetland reclamation is one of the most important ways of changing land suitability for crop growth by humans. Historically, land suitability for cultivation in many wetland areas gradually expanded with continuous wetland reclamation (Davidson 2014; Gedan et al. 2009; Martín-Antón et al. 2016; Waz and Creed 2017; Bao et al. 2019; Verhoeven and Setter 2010). In these areas, the distribution of modern croplands is larger than that of historical croplands (e.g., Martín-Antón et al. 2016; Nguyen et al. 2016; Bao et al. 2019). That is, many modern croplands were unsuitable for farming before the wetlands were reclaimed (e.g., Gedan et al. 2009; Brinson and Malvárez 2002). As one of the important methods of wetland reclamation, polders have been widely distributed in many regions of the world (Segeren 1983; Martín-Antón et al. 2016), such as the coastal lowlands of the Netherlands (e.g., Hoeksema 2007), the Ganges Delta of Bangladesh (e.g., Auerbach et al. 2015), and the Middle-Lower Yangtze River Plain of China (e.g., Wang et al. 2016). Polders are cropland systems with dikes and drainage facilities in low-lying areas such as wetlands (Segeren 1983). Through polders, uncultivable wetlands are drained and transformed into arable land, which leads to the expansion of land suitable for crops (Segeren 1983). Thus, the study of cropland area allocation in polder areas could provide a case for better understanding the impacts of changing land suitability for crops on spatially explicit reconstructions.

The Dongting Plain (DTP) is the most typical area of polder distribution in the Middle-Lower Yangtze River Plain of China (Han 2012; Marks 2011; Zou et al. 2013). In the DTP, large-scale polders have been constructed since the late seventeenth century (Mei et al. 1995; Gong 1996; Li 2014; Wang et al. 2016). The land suitable for crops gradually expanded, following constant polders construction over the centuries. The DTP could provide a case study of the impact of changing land suitability for crops on spatially explicit reconstructions. In this study, the spatiotemporal changes in polders and cropland area in the DTP were reconstructed over the past 300 years, and the cropland cover was reconstructed based on polder expansion in a spatially explicit reconstruction.

Study area

The DTP is in Hunan Province, which is located in south of the middle reaches of the Yangtze River (28°–30° N, 111°–114° E). The area to the north is limited by the Yangtze River, and the area to the east and west is limited by mountains. The area is 2.45×10^4 km^2, covering 11.56% of the total area of Hunan Province. The study area falls within the subtropical humid climatic zone (with an annual mean precipitation of more than 1200 mm and a mean temperature of more than 16 °C), and most elevation ranges in this area are less than 50 m above sea level (a.s.l.) (Fig. 1). The more favorable climatic and landform conditions for agricultural development resulted in the DTP being an important food production area (Mei et al. 1995; Wang et al. 2016).

There are many rivers and lakes in the DTP, and these water bodies affect land reclamation. Dongting Lake is located in the middle of the DTP and is the second largest freshwater lake in China; it was the largest freshwater lake in China at one time. Rivers, such as the four channels of the Yangtze River (FCs) and the Four Rivers (FRs), flow into Dongting Lake. The FCs, including the Hudu River, Ouchi River, Songzi River, and Tiaoxian River (which was blocked in 1958), flow from the

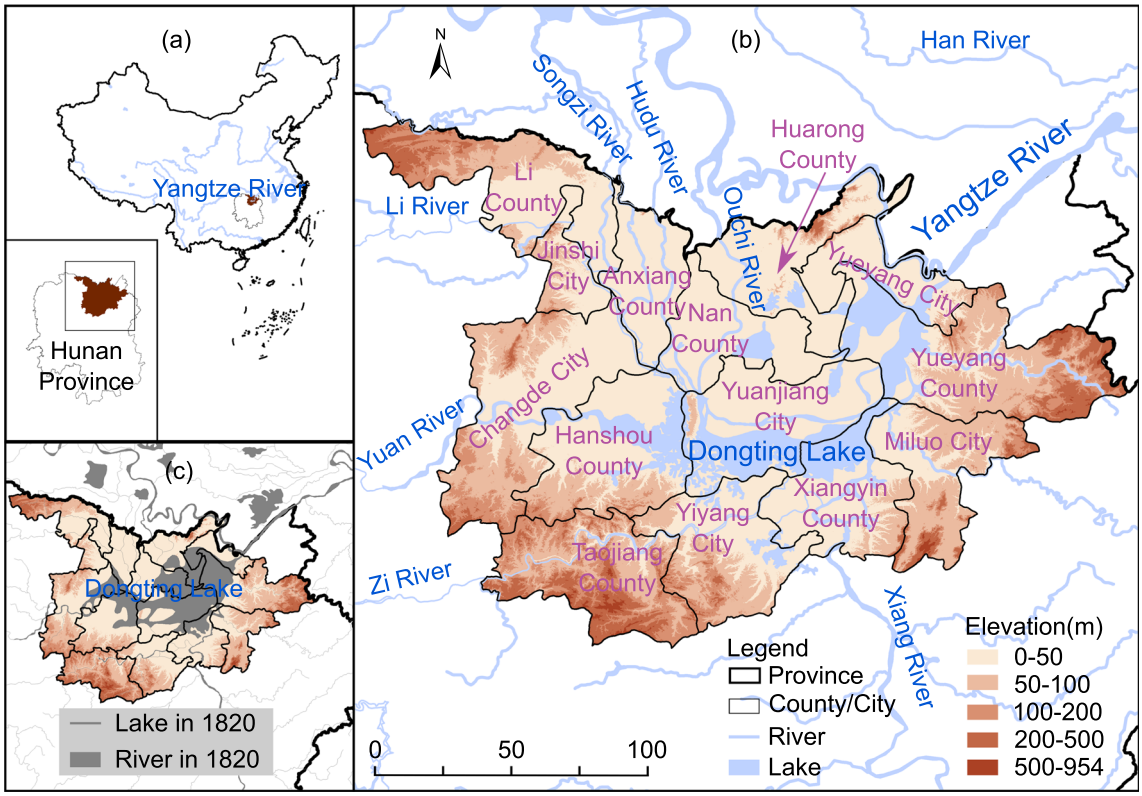

Fig. 1 Study area: **a** geographic locations of the Dongting Plain area in China; **b** the modern administrative boundaries, rivers, and lakes in the Dongting Plain; and **c** the rivers and lakes in 1820 (data were from https://dataverse.harvard.edu/dataverse/chgis_v6)

north into Dongting Lake. The FRs include the Xiang River, Zi River, Yuan River, and Li River, and they flow from the south and west into Dongting Lake, respectively. Between 1951 and 2008, the annual average runoff of Dongting Lake was 2.897×10^{11} m^3, and 32.44% and 57.96% of the total runoff came from FCs and FRs, respectively (Li 2014). The annual average sediment discharge of Dongting Lake is 1.54×10^8 t, and 81.67% and 18.33% of the total sediment discharge came from FC and FR, respectively (Li 2014).

Data and methods

To reconstruct cropland cover change in a spatially explicit reconstruction over the past 300 years, three sections were completed using different data, including reconstrction of land suitable for crops indicated by polders, reconstruction of cropland areas, and allocation of cropland areas into the grids (see Fig. 2). Notably, this study centered on historical cropland changes and discusses historical changing land suitability for crops on spatially explicit reconstruction. Additionally, this study aided in improving the global historical cropland datasets based on case analyses. Hence, this study did not pay much attention to modern cropland changes (after 1949).

Data

For the reconstruction of polders indicative of land suitable for crops, remote sensing images, maps, and local gazetteers were used in this paper. The remote sensing images were obtained from Google Earth (http://earth.google.com), with a spatial resolution of 4 m, and the images are the 2010s. The maps were obtained from the books of *The historical atlas of Dongting Lake* (Department of Land and Resources of Hunan Province 2011) and *The atlas of polder in Dongting Lake district in Hunan Province* (Department of Water Resources of Hunan Province 1987). The local gazetteers include three categories. The modern gazetteers of the water conservancy were obtained from the books of *The gazetteer of water conservancy of Dongting Lake district* (Compilation Office of Water Resources of Hunan Province 1985) and *The gazetteer of water conservancy of Dongting Lake* (Department of Water Resources of Hunan Province 1989). The modern county gazetteers, including districts, counties, and county-level cities, were obtained from the library. Additionally, the local gazetteers of the Qing dynasty were obtained from the National Digital Library of China (http://x.wenjinguan.com/).

For the reconstruction of historical cropland areas that changed over time, historical documents were available (Ye et al. 2009; Yang et al. 2016; He et al. 2017; Li et al. 2018).

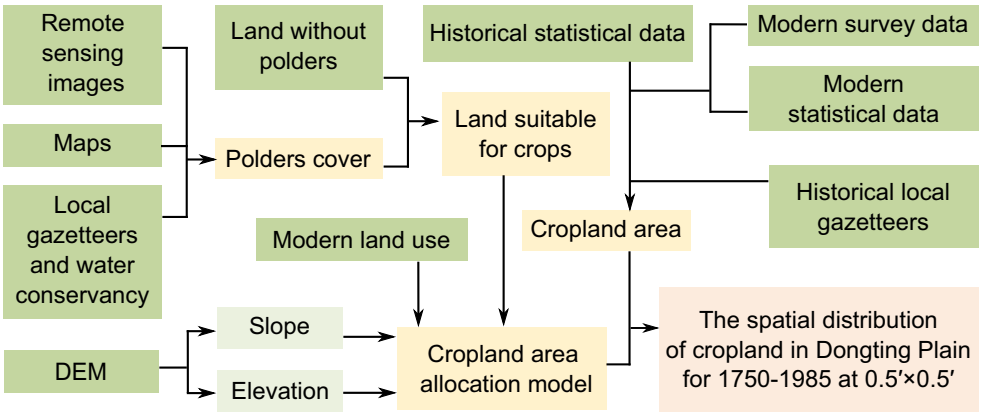

Fig. 2 Flowchart depicting the analytical outline of this study. Green boxes indicate data, and yellow boxes and red box indicate results

Then, the diversity of the data was analyzed to produce a unified cropland series (Ye et al. 2009; Ye et al. 2015; Wei et al. 2016). According to previous studies (Ye et al. 2009; Ye et al. 2015; Wei et al. 2016), historical local gazetteers were used to reconstruct the historical cropland area; historical statistical data, modern statistical data, and modern survey data were used to calibrate and reconstruct cropland areas. All data were at the county-level scale, and all statistical data meant the data based on statistics. The modern statistical data were obtained from the book of *The economy of Hunan over the past 50 years*, which recorded cropland statistical data on an annual basis (Zhang et al. 1999). The modern survey data were obtained from the Datasets of Land and Resources of China (http://mlr.gov.cn/), which recorded cropland survey data in the 1980s. The historical statistical data were obtained from the library and included the books of *Land utilization in China statistics in 1930* and *Summary statistics agricultural tax of Hunan in 1941*. The historical local gazetteers were obtained from the National Digital Library of China (http: //x.wenjinguan.com/). Moreover, the administrative divisions of the Qing dynasty were obtained from the Chinese Historical Geographic Information System (https://dataverse.harvard.edu/dataverse/chgis_v6).

The cropland areas of the administrative divisions were allocated into grids using the cropland area allocation model (Li et al. 2016; Wei et al. 2019). The model includes some natural factors that affect crop growth and cropland spatial distributions, such as temperature, precipitation, elevation, and slope (Li et al. 2016; Wei et al. 2019). The temperature and precipitation data were obtained from the Resource and Environment Data Cloud Platform (http://www.resdc.cn/Default.aspx), with a spatial resolution of 500 m × 500 m. The elevations were obtained from SRTM (http://srtm.csi.cgiar.org/SELECTION/inputCoord.asp), with a spatial resolution of 90 m × 90 m, and the slope was calculated using the DEM. Moreover, modern land use is a factor in the cropland area allocation model, as modern land use represents the potential maximum cropland area fraction (e.g., Wei et al. 2019). Modern land use data were obtained from GlobeLand30 (http://www.globallandcover.com/GLC30Download/index.aspx), with a time section of 2000 and a spatial resolution of 30 m × 30 m. Finally, a new factor was used in this study, namely, the land suitable for crops, which was the result of the reconstruction conducted in this study.

Polder change reconstruction

According to the existential timeline, the polders in the DTP were divided into two types, current polders and disappeared polders. The two types of polders were reconstructed in different ways. Current polders contain many different polders from different historical periods, which accumulated with the evolution of added, reconstructed, and merged polders over the centuries. For reconstruction of the spatiotemporal extent of the current polders, remote sensing images, maps, and local gazetteers were used to extract the polder pitches, the polder names, and the times of polder constrction, respectively. Dikes and dike relics can be used as indicators to distinguish between polders from different historical periods. These indicators include dikes, continuous settlements, relatively high roads, ancient channels, continuous ponds, and croplands formed by river blockages. Using visual interpretations, current polders can be distinguished as polder patches because these indicators can be identified in remote sensing images.

Reconstructions of the spatiotemporal extent of the current polders involved the following steps. First, in the remote sensing images, the study area was subdivided into a modern polders cover area and other land without polders. The former is distributed with polders and the latter has no distribution. Second, using visual interpretation, the modern polder area was distinguished from different polder patches by dikes and dike relics. Third, the polder patches were given the original polder names from maps. Fourth, the polder patches were marked with the times of constrction from local gazetteers. After this processing, the current polder area was reconstructed.

The disappeared polders were polders that once existed but do not currently exist, as they are submerged in lakes and rivers and cannot be identified in remote sensing images. Disappeared polders mainly disappeared since the late nineteenth century, and the south Dongting Lake and west Dongting Lake areas are relatively concentrated with disappeared polders (Li 2014). The locations and extent of the disappeared polders were obtained from previous studies, modern gazetteers of the water conservancy, and maps (e.g., Li 2014). Moreover, the times of construction and disappearance were obtained from local gazetteers

Furthermore, the current polders and disappeared polders were merged in accordance with their corresponding periods. The polders from different historical periods were merged into land without polders. Hence, a spatiotemporal reconstruction of the land suitable for crops was made.

Cropland area reconstruction

The cropland area changes at the county level were reconstructed. Notably, modern survey data of cropland areas, from approximately 1985, were directly used in this study because the modern survey data are accurate (Ye et al. 2009; Ye et al. 2015; Wei et al. 2016; Yuan et al. 2017). There are 17 districts, counties, and county-level cities in this area. To easily employ the use of statistics, these areas were merged into 14 county levels in this study, including Yueyang City (Yueyanglou District and Junshan District), Xiangyin County, Miluo City, Yueyang County, Huarong County, Changde City (Dingcheng District and Wuling District), Hanshou County, Anxiang County, Lixian County, Jinshi County, Yiyang City (Ziyang District and Heshan District), Nanxian County, Taojiang County, and Qijiang City (see Fig. 1).

Cropland area calibration during 1912–1949

This cropland area of the Republic of China period (1912–1949) was calibrated (Ye et al. 2009; Wei et al. 2016). First, a correlation analysis of the modern statistical data from 1985 and the modern survey data from the 1980s was conducted. The correlation was highly significant ($r = 0.939$; $p < 0.01$). Second, considering the correlation analysis results, a linear regression function between the modern statistical data and modern survey data was developed as follows:

$$Y = 1.25X, R^2 = 0.8756$$

where X is the modern statistical data of 1985 and Y is the modern survey data of the 1980s.

Finally, the historical statistical data were calibrated using the linear regression function, which provided the cropland areas in 1930 and 1941.

Cropland area reconstruction before 1911

In the Qing Dynasty (1644–1911), considering the data coverage and regional socioeconomic history, the time sections of the reconstruction were identified as 1750 and 1850. First, the cropland area records were collected from historical local gazetteers. Second, cropland area records were disposed of according to the methods of a previous study (Wei et al. 2015). The cropland area was converted from traditional units into metric units as 1 Qingmu = 0.9216 Mu = 0.9216/1500 km^2. The unregistered cropland area accounted for 23% of the total cropland area according to a previous study (Gong 1996). Finally, the cropland areas of 1750 and 1850 were reconstructed at the county level.

The unified cropland area change production

Notably, the cropland areas of certain time sections lacked information regarding the corresponding period to the land suitable for crops. The cropland areas of 1911 and 1949 needed to be interpolated considering the socioeconomic history and environmental change. First, the cropland area of 1911 was estimated with a linear interpolation between the cropland areas of 1850 and 1930. The cropland was estimated above on the assumption that the cropland change linearly increased and the average growth area per annum was changeless from 1850 to 1930. Second, the cropland area of 1941 was used as a substitute for the cropland area of 1949, because the cropland area of 1941 reflected a number with more cropland area, and there had been many periods of unrest from 1941 to 1949. The cropland area of 1949 was in a growing stage, and the regional government organized a large-scale reclamation after 1949, which resulted in an increasing number of croplands after 1949 and more than that of 1949. This meant that the cropland area of 1941 was the closest to 1949 in all current obtainable cropland numbers. Hence, using calibration and interpolation, the unified cropland area change was reconstructed over the past 300 years.

Cropland area allocation

To allocate the total cropland area into grids, we used a cropland area allocation model created by previous studies (e.g., Li et al. 2016; Wei et al. 2019). The cropland area allocation model included some natural factors (e.g., slope, elevation, temperature, and precipitation) that influenced crop growth and cropland spatial distributions. However, the characteristics in this area needed to be considered when allocating, and some factors needed to be adjusted in the model. For the cropland spatial distributions in this area, the influence of temperature and precipitation were almost negligible, and the influence of elevation on the cropland was different between land with polders and land without polders. The land

suitable for crops played an important role in the spatiotemporal distribution change of cropland over time. Multiple factors were calculated, and they were analyzed with a spatial resolution of 0.5′ × 0.5′.

Temperature and precipitation, which have been used as a factor in existing studies, should reflect climates that suitable for cultivation (e.g., Li et al. 2016; Wei et al. 2019). However, this region is characterized by a subtropical humid. The accumulated temperature (above 10 °C) during the growing period is 4299.3–5724.4 °C, and the annual mean precipitation is 1224.7–1525.9 mm. The suitable temperatures and abundant precipitation have not changed significantly over the last few hundred years according to previous studies (e.g., Hao et al. 2012; Wu et al. 2010). They meet the growth requirements of plants. Moreover, to balance the spatiotemporal distribution differences of precipitation, humans have built many irrigation systems and water utilities since antiquity. Hence, the temperature and precipitation values were set to one in the cropland area allocation model because these variables had nearly no influence on cropland distribution.

Based on previous studies, the smaller the slope mean is, the better conditions for agricultural development, resulting in more fraction under cropland area (e.g., Li et al. 2016; Wei et al. 2019). The slope was standardized in the cropland suitability for cultivation analyses. Meanwhile, the influence of elevation on agricultural development had a spatial difference in the DTP. In the land without polders of DTP, the lower elevation had better conditions for agricultural development and was standardized in this analysis, just as with the slope analyses. The opposite analysis was in the polders cover area. The main reason was that drainage was difficult at lower altitudes (Mei et al. 1995; Li 2014; Wang et al. 2016). These areas had lower fractions under the cropland area because of many puddles. The elevation suitability was calculated according to the order of the elevations from high to low. Notably, the suitability of the lowest elevation was set to 0.80 in this study, because the cropland areas in dozens of polder were close to 1 km^2 (this area is approximately equal to one grid) and made up approximately 80% of the total area according to our statistical results. This meant that the elevation suitability in the cropland area allocation model was usually greater than 0.80.

In addition, modern land use was used to show the historical potential of the cropland fraction (e.g., Wei et al. 2019). The potential cropland fraction included the proportion of modern cropland, the proportion of modern construction land, and the proportion of modern wetland in this area. The main reason the modern construction land increased was because of urbanization, which occupied croplands, and part wetlands increased because of cropland abandonment (e.g., restoration polders). Apparently, many wetlands were calculated as croplands, even though these wetlands were unrelated to croplands. In fact, wetlands were excluded from the land suitable for crops. Hence, the historical potential cropland fraction was only applied in land suitable for crops. The Wcrop′(i) of the historical potential cropland fraction weight of grid cell i is as follows:

$$Wcrop'(i) = Wcrop(i) + Wcon(i) + Wwet(i) \quad (1)$$

where Wcrop(i), Wcon(i), and Wwet(i) are the cropland, construction land, and wetland fraction weights of grid cell i, respectively.

The cropland area allocation model includes the historical potential cropland fraction and land suitable for crops, elevation, and slope. The Suit(i) of cropland suitability for cultivation weight of grid cell i is as follows:

$$Suit(i) = Wsuitable(i) \times Wcrop'(i) \times \mathrm{E}'(i) \times S'(i) \quad (2)$$

where Wsuitable(i) is the land suitable for crops weight of grid cell i and E′(i) and $S'(i)$ are the elevation and slope standardized value weights of grid cell i, respectively.

Therefore, in the k_n of the county level, the ratio of cropland area $w(i)$, cropland area Crop(i), and cropland fraction CF(i) of grid cell i are as follows:

$$w(i) = Suit(i)/\sum_{i=1}^{i} Suit(i) \quad (3)$$

$$Crop(i) = w(i) \times A(k_n) \quad (4)$$

$$\mathrm{CF}(i) = Crop(i)/Area(i) \quad (5)$$

where n is the grid number of the k_n of county level, $A(k_n)$ is the cropland area in k_n of county level, and Area(i) is the cropland area of grid cell i.

Finally, using the cropland area allocation model, the cropland area was allocated into grids, and the spatiotemporal of cropland cover were mapped with a spatial resolution of 0.5′ × 0.5′.

Cropland fraction comparison

To validate the results of this study, GlobeLand30, which is a remote sensing land cover product, was used as a standard. Using ArcGIS 10.2, the cropland area of GlobeLand30 with a spatial resolution of 30 m × 30 m was counted as the cropland fraction with a spatial resolution of 0.5′ × 0.5′. Notably, the cropland fraction of 2000 in this study was comparison. The comparison formula is as follows:

$$Differences(i) = \mathrm{CF}(i) - \mathrm{CFG}(i) \quad (6)$$

where Differences(i) is the absolute difference between this study and the GlobeLand30 in grid i, and CF(i) and CFG(i) are the cropland fractions of grid i in this study and GlobeLand30, respectively.

In addition, to better understand the impact of the changing land suitable for crops in the spatially explicit reconstruction, this study and HYDE 3.2 were compared. The cropland fraction was compared with a

spatial resolution of 5′ × 5′. The comparison formula is as follows:

$$Differences(i) = \mathrm{CF}(i) - \mathrm{CFH}(i) \quad (7)$$

where Differences(i) is the absolute difference between this study and the HYDE 3.2 in grid i, and CF(i) and CFH(i) are the cropland fractions of grid i in this study and HYDE 3.2, respectively.

Results

The land suitable for crops change

The land suitable for crops in the DTP changed significantly over the past 300 years (see Fig. 3). In terms of quantity, the proportions of land suitable for crops in 1750, 1850, 1911, 1949, and 1985 accounted for 68.24%, 68.24%, 75.05%, 80.59%, and 85.10% of the total area, respectively. After 1850, change in the land suitable for crops occurred. The proportions of land suitable for crops gradually increased; as in 1911, 1949, and 1985, they were 1.10, 1.18, and 1.25 times that in 1750, respectively. In other words, the land suitable for crops in 1850, 1911, and 1949 was equivalent to 80.19%, 88.19%, and 94.70% that of 1985, respectively. Simultaneously, lakes were replaced by croplands. From 1750 to 1985, the area of land suitable for crops increased 4130.52 km^2, which was equivalent to 68.83% of Dongting Lake area in 1825 (Zou et al. 2013). Considering the spatial extent, the land suitable for crops expanded from the periphery to a concentration in the center. The largest amount of land suitable for crops was in the center of the area. As the land suitable for crops increased, the unsuitable land that could not be cultivated was reduced. The land unsuitable for crops in 1911, 1949, and 1985 amounted to 78.56%, 61.11%, and 46.91% that of 1750, respectively.

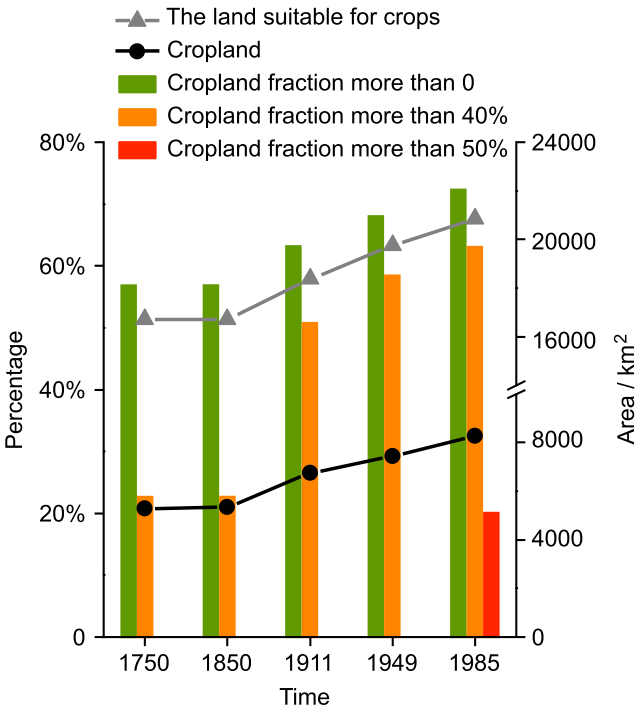

Fig. 3 The land suitable for crops and the cropland area of the DTP for 1750–1985. The black line indicates the cropland area, and the gray line indicates the area of land suitable for crops. The green boxes indicate the proportion of grids with cropland, and the orange and red boxes indicate the proportion of grids with a high cropland fraction

The change in land suitable for crops was closely connected with the polder change over the past several hundred years. The polders experienced great changes due to changing relationships between rivers and lakes. The most important changes occurred in the middle and late nineteenth century in two main aspects. On the one hand, the northern Dongting Lake area deceased in size due to a large amount of siltation. The reason for this siltation was that the Yangtze River breached in 1852 and 1870 and developed into the Ouchi and Songzi Rivers in 1860 and 1873, respectively (Zou et al. 2013; Li 2014). The two rivers carried large quantities of sediment into the lake basin. Statistically, the sediment discharge in the Ouchi and Songzi Rivers made up 73.16% of the total sediment discharge (Li 2014). As a result, the land suitable for tillage expanded in the northern area. On the other hand, Dongting Lake moved southward because the lake eroded the land (Zou et al. 2013). The polders that were originally distributed in this location were damaged, which expanded the land unsuitable for cultivation in the southern area.

The total cropland area change

Along with the changing land suitable for plants, the cropland area also changed in the DTP (see Fig. 3). The cropland areas decreased in the areas that experienced riots in the middle of the seventeenth century, and the cropland area grew when society reached a stable state after the late seventeenth century (Mei et al. 1995; Gong 1996). Over a long development period, the cropland area reached 5291.97 km^2 in 1750, which constituted 21.60% of the total area. Since then, the cropland remained stable for a long time. The cropland area in 1850 was 5326.50 km^2, which was only 0.65% higher than the area in 1750. After 1850, the cropland area increased as the number of polders increased. The cropland area increased from 6731.87 km^2 in 1911 to 7423.03 km^2 in 1949, which was equivalent to 127.21% and 140.27% that of 1750, respectively. After 1949, the cropland area increased significantly with the comprehensive integration of various factors (Li 2014). Until the 1980s, the cropland area began to decrease due to urbanization and environmental protection (Li 2014; Wang et al. 2016). In 1985, the cropland area reached 8256.80 km^2, which covered 33.70% of the total area and was equivalent to 156.03% that of 1750. In the time that followed, the cropland area decreased because of factors, such as

urbanization and environmental policy. The cropland area in 2000 was 7799.52 km^2, which was equivalent to 94.46% that of 1985.

The spatiotemporal change in cropland cover

The spatiotemporal changes in the grids with cropland fraction showed significant differences from 1750 to 1985 (see Fig. 4). Moreover, a substantial increase over the study period was found in the northern DTP, but a decrease occurred in the southern DTP (see Fig. 5).

From 1750 to 1985, the spatial distribution of the grids with cropland fraction showed four characteristics, accounting for 32.16%, 40.14%, 26.02%, and 1.69% of the total grids, respectively (see Fig. 5a). First, the cropland fraction increased by more than 30%. This change was attributed to the development of polders. These grids were distributed mainly in the central area along the banks of the Ouchi and Songzi Rivers. Second, the cropland fraction increased by more than 1%, but not more than 10%, mainly due to reclamation in the mountains. These grids were located in the surrounding mountains in this area. Third, the cropland fraction remained the same or changed by less than 1%. These grids were located in the modern Dongting Lake and other places because these grids have been difficult to cultivate from ancient times until now. Meanwhile, grids with cropland fractions were also too high to continue to increase as these areas had a long land use history (Mei et al. 1995; Li 2014). Last, the cropland fraction decreased by more than 20% as the cropland was submerged by the floods that occurred in these grids. These grids were distributed in the modern Dongting Lake and modern Ouchi and Songzi Rivers.

Different performances in these changes were found during different periods (see Fig. 4). In 1750, the cropland fraction was low. The proportion of grids with a cropland fraction of 30–40% was the highest, accounting for 27.24% of the total, while the proportion of grids with a cropland fraction of more than 40% was only 22.73% of the total. The grids with high cropland fraction were concentrated mainly in the northern, southern, and western parts of the DTP, especially in the FR deltas. Moreover, the area was reclaimed earlier and concentrated within towns (Mei et al. 1995; Gong 1996). The grids

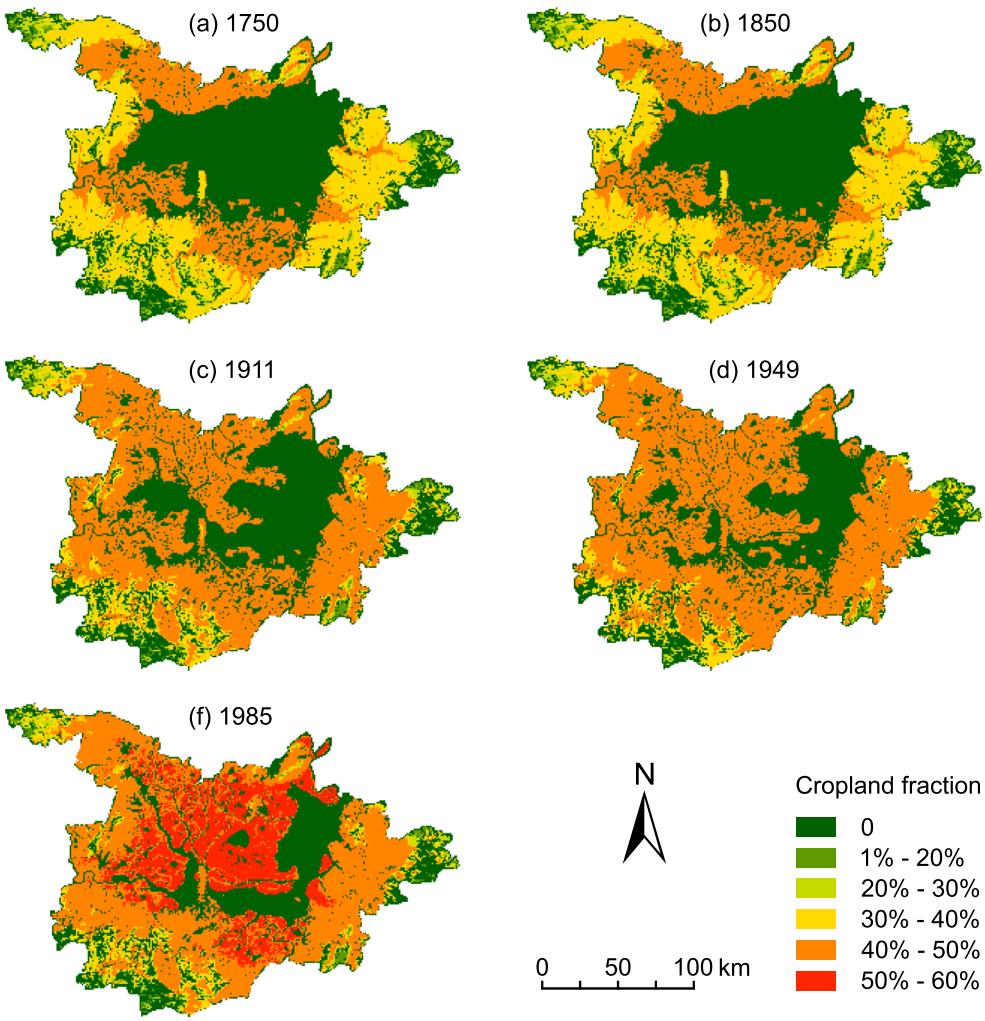

Fig. 4 The spatial distribution of cropland fractions in the Dongting Plain for 1750–1985 with a spatial resolution of 0.5′ × 0.5′. From green to red indicates a gradual increase in the cropland fraction

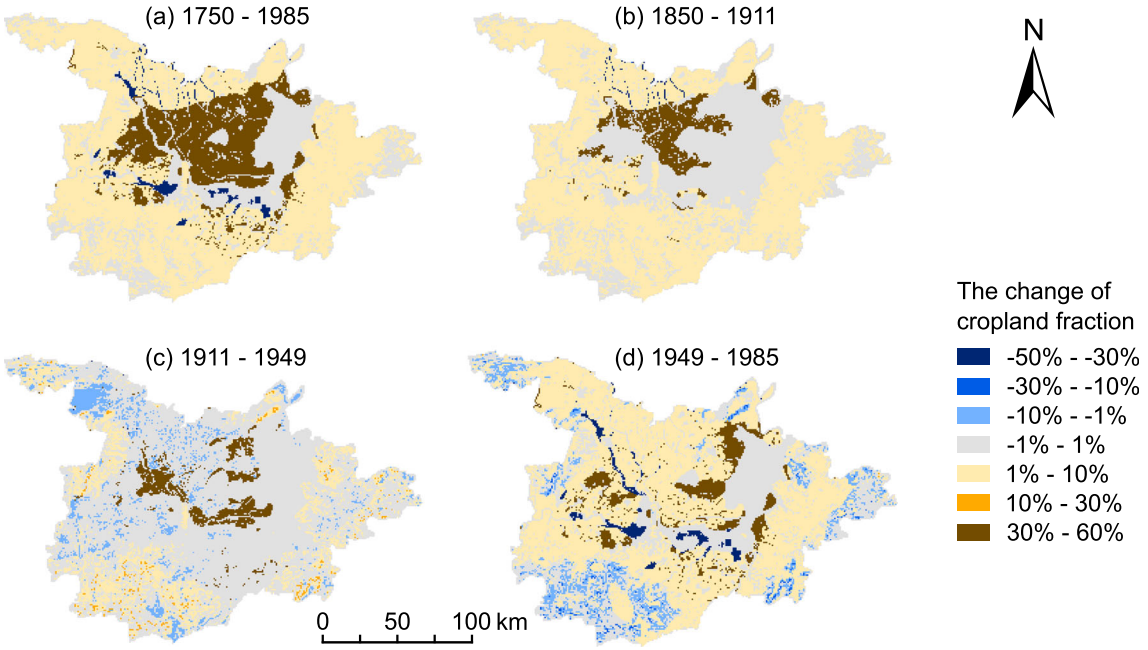

Fig. 5 Cropland fraction changes in the Dongting Plain between 1750 and 1985 with a spatial resolution of 0.5′ × 0.5′. The blue and brown indicate decreased cropland fractions and increased cropland fractions in the grids, respectively

without a cropland fraction were located mainly in the central area, which was the extent of Dongting Lake at that time.

The spatial distribution of grids with cropland fractions remained constant between 1750 and 1850. The main reason was that reclamation had reached saturation under the conditions at the time, and the cropland area changes were less from the mid-eighteenth century to the mid-nineteenth century (Mei et al. 1995; Gong 1996). A similar phenomenon occurred in other areas. For instance, the cropland fraction was nearly the same in the flat plains of North China from the eighteenth to the nineteenth century (Wei et al. 2015; Wei et al. 2019).

The cropland fraction increased significantly from 1850 to 1911. The proportion of grids with a cropland fraction of more than 40% was the highest, covering 50.82%. The girds that increased in the cropland fraction were mainly affected by two events. On the one hand, cropland fractions significantly increased in the central area because humans constructed many polders on the rich sediment that was carried by the Ouchi and Songzi Rivers. (Mei et al. 1995; Li 2014). On the other hand, the grids with cropland fractions increased in the surrounding mountains as humans reclaimed the mountainous areas (Mei et al. 1995; Lu 2016). The former increased the cropland fraction by more than 30%, while the number only occupied 6.69% of the total grids. The latter increased the cropland fraction by less than 10%, covering 56.49%. The grids with a cropland fraction were reduced and mainly concentrated in the northern area, accounting for only 0.32% because the croplands were submerged in the Ouchi and Songzi Rivers. Compared with several of the periods, the cropland cover appeared to show the most distinct change between 1850 and 1911.

The proportion of grids in which the cropland fraction remained unchanged or increased by less than 1% was 71.08% in 1911–1949. The proportion of grids with an increased cropland fraction occupied 21.84%. The grids in which the cropland fraction increased by more than 30% constituted only 4.92%. The proportion of grids in which the cropland fraction increased by 1–10% comprised 15.78%. Following land reclamation, the proportion of grids with a cropland fraction of more than 40% was 58.47% in 1949.

From 1949 to 1985, the grids with cropland fractions increased substantially. There were two grid types with increased cropland fractions, namely, those that increased less than 10% and those that increased more than 30%, accounting for 52.40% and 6.12%, respectively. Among the latter, the proportion of grids in which the cropland fraction increased more than 50% occupied 4.30%. These grids were located in areas that had been occupied by lakes, such as eastern Dongting Lake, Datong Lake, and western Dongting Lake. Croplands dominated the lake areas in the grids because of large-scale lake reclamation. In addition, 9.29% of the grid proportions experienced a significant decrease in the cropland fraction because the polders were damaged by floods. Additionally, the proportion of grids in which the cropland fraction remained unchanged covered 32.17%. Thus, the grids with cropland fractions of more than 40% occupied 63.12% of the total grids in 1985. The grids with a cropland fraction of more than 50%, covering 20.13%, were distributed along the shores of lakes and deltas of rivers.

Discussion

Comparison with satellite-based data

Compared with GlobeLand30, the grids with cropland fractions allocated by the cropland area allocation model were validated. By comparison, a significant positive correlations were found between this study and GlobeLand30 ($r = 0.643$, $p < 0.01$). This correlation meant that the results of this study could reflect the actual cropland cover in a spatially explicit reconstruction (see Fig. 6). The results showed a generally concentrated distribution. The proportion of grids with differences of between − 20 and − 60% was close to half of the total grids (46.52%), and it conformed to the general rule that the cropland fraction obtained by the cropland area allocation model was lower than the satellite-based data based on previous studies (e.g., Li et al. 2016). However, some differences still existed between grids. The results showed that the proportion of grids with differences of more than zero and less than zero made up 18.27% and 60.57%, and they were located in the plain and mountain areas, respectively. This finding indicated that the cropland fraction was overestimated and underestimated in the mountains and plains in this study, respectively.

In addition, there were two kinds of misinterpretations in the GlobeLand30, which affected the results comparison. The first misinterpretation was that cropland was interpreted as other land use categories, leading to the results comparison having a low correlation. For example, GlobeLand30 interpreted the modern Caowei River Delta in the eastern Dongting Lake as cropland. However, in reality, the area was grassland or wetland based on other research (e.g., Wang et al. 2016), and this area constituted 0.95% of the total grids. On the other hand, other land use categories were interpreted as cropland. For example, GlobeLand30 interpreted the Minzhu Polder of Yiyang, a polder with some croplands (e.g., Wang et al. 2016) located southern of the Dongting Lake, as waters. These grids covered 0.39% of the total grids.

Comparison with HYDE 3.2

Many historical cropland cover changes in the areas with abundant wetlands have been reconstructed in a spatially explicit reconstruction. However, few of these studies have allocated historical cropland area in light of changing land suitability for cultivation over times. In a comparison with HYDE 3.2 (Goldewijk et al. 2017), the latest version of the HYDE, difference in changes in the land suitable for crops were understood on spatially explicit reconstruction.

First, the total cropland area quantities were compared in the study area. The cropland area of HYDE at each time point was 68.72%, 119.63%, 80.46%, 86.20%, and 78.77% in this study. The HYDE values were generally low, approximately 80% in this study. This divergence was caused by different data sources. HYDE allocated the Chinese provincial cropland area based on previous studies into grids (Li et al. 2016). In this paper, the cropland area at the county level was used to reconstruct.

The HYDE values were lower in 1750 than in this study, while they were higher in 1850 than in this study. The reason was that there was an obvious increase in provincial cropland areas from 1750 to 1850 according to previous studies (Li et al. 2016). HYDE indicated that the change had occurred

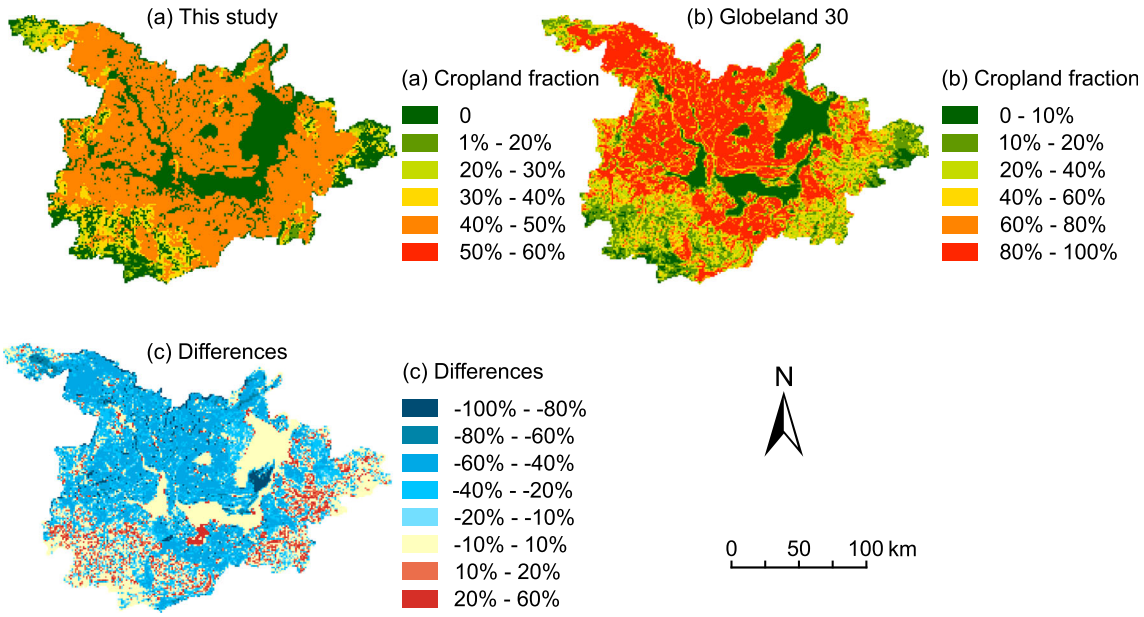

Fig. 6 Comparisons between satellite-based data and this study with a resolution of 0.5′ × 0.5′. **a** Reconstructed cropland cover for 2000. **b** Satellite-based crop cover for 2000. **c** Differences between **a** and **b**

in all of Hunan. However, historians have stated land reclamation occurred in the DTP in the mid-eighteenth century but not in the mid-nineteenth century (Gong 1996; Lu 2016). The cropland area change was less from the mid-eighteenth century to the mid-nineteenth century as reclamation had reached saturation under the conditions at the time (Mei et al. 1995; Gong 1996). There were significant within provincial differences. Thus, research is also needed to quantitatively reconstruct the cropland area at the county level to reconstruct cropland cover with a higher precision and spatial resolution (Wei et al. 2015).

Then, the spatial distinction of the grids with cropland fraction was compared in the study area. Given that cropland cover changes occurred an abrupt change in the late nineteenth century, the grids with cropland fraction were compared in the years 1850, 1911/1910, and 1949/1950 (see Fig. 7). The proportions of grids suitable for crops with a spatial resolution of 5′ × 5′ were 80.79%, 88.67%, and 93.10% of the total grids in the years 1850, 1911, and 1949, respectively. A similar trend was found in terms of land suitable for crops with different spatial resolutions. In addition, there were a higher percentage of grids with a spatial resolution of 0.5′ × 0.5′. The lower the spatial resolution was, the lower the difference that was found. This result meant that the difference in the land suitable for crops could be ignored at low resolutions.

The land unsuitable for crops decreased as the land suitable for crops grew. The numbers of grids unsuitable for crops were 78 in 1850, 46 in 1910/1911, and 28 in 1949/1950, which constituted 19.21%, 11.33%, and 6.90% of the total grids, respectively. As the study period reached modern time (1980s), smaller differences between HYDE and this study in the land suitable for crops were observed. In the land unsuitable for crops, the proportions of grids that were allocated as cropland by HYDE 3.2 in 1850, 1910, and 1950 were 93.59%, 89.13%, and 82.14% of the total grids unsuitable for crops. This result meant that the reliability of these grids was uncertainty when a spatially explicit reconstruction of cropland change was carried out in this area.

By comparison, there were three results that were observed, namely, a difference of more than 1%, a difference of less than − 1%, and a minimum difference. In 1850, the first and second results comprised 40.89% and 54.93% of the total grids, respectively. The former was mainly concentrated in the northwest, southwest, and east areas, especially the southwest area. The latter was mostly concentrated in the middle area, and a small part was concentrated in the northeast area. In approximately 1911, the first result and second result accounted for 61.33% and 33.25% of the total grids, respectively.

A difference of less than − 1% indicated that HYDE overestimated the cropland fraction. Most of these areas were considered as land unsuitable for tillage. In 1850, HYDE interpreted the grids belonging to land unsuitable for crops as 17.98% of the total grids, and the cropland area occupied 21.73% of the total area. In approximately 1911, HYDE interpreted the grid number and cropland area as 10.10% and 11.51%, respectively. The reason why these grids had

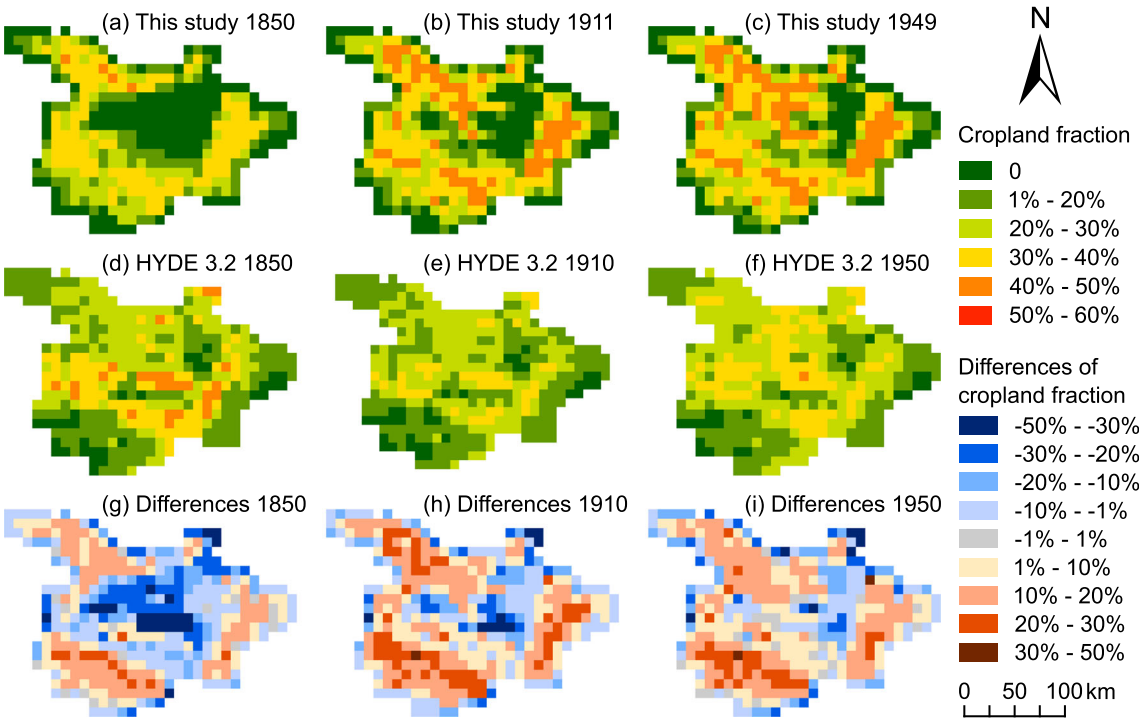

Fig. 7 Comparison between this study and the HYDE 3.2 dataset for 1850, 1810/1911, and 1950/1949 with a resolution of 5′ × 5′. **a**, **b**, and **c** were reconstructed in this study; **d**, **e**, and **f** were reconstructed by HYDE 3.2; **g**, **f**, and **i** are differences between this study and the HYDE 3.2

higher cropland fractions was that more landform conditions (e.g., flat) for agriculture were in these grids (Mei et al. 1995; Gong 1996; Wang et al. 2016).

In approximately 1949, the grids with differences of more than 1% and less than − 1% accounted for 60.59% and 33.50%, respectively. The gap narrowed between this study and HYDE. Using the grids with differences of between − 10 and 10% and grids between − 20 and 20% to illustrate the point, the grids accounted for 44.58% and 84.98% of the total grids in approximately 1949, but covered 41.63% and 79.06% in approximately 1911, respectively. Hence, the differences were gradually reduced over time. This difference was caused by the total quantity of the cropland area and not changes in land suitability for crops.

Conclusions

Cropland area changes were reconstructed at the county level in the DTP over the past 300 years, and the historical cropland area was allocated into grids with a spatial resolution of 0.5′ × 0.5′. Cropland allocation accounted for changes in land suitable for crops. The results showed the following:

(1) Land suitable for crops in the DTP changed significantly due to environmental changes and human activities over the past 300 years. The land suitable for crops covered 68.24% of the total area in 1750. The change occurred and expanded from the periphery to the center after 1850, expanding markedly in the center area. The land suitable for crops in 1911, 1949, and 1985 was 1.10, 1.18, and 1.25 times that of 1750, respectively. Meanwhile, the land unsuitable for crops was reduced, and the land unsuitable for crops in 1985 was equivalent to 46.91% in 1750.

(2) The cropland area also changed in the DTP. The total cropland area reached 5291.97 km^2 in 1750, accounting for 21.60% of the total area. The cropland remained stable in the long term, which was only 0.65% higher in 1850 than in 1750. After 1850, the cropland increased the number of polders grew. The cropland areas in 1911, 1949, and 1985 were equivalent to 127.21%, 140.27%, and 156.03% that of 1750, respectively.

(3) Four factors had important effects on cropland cover changes between 1750 and 1985. First, the development of polders led to a more than 30% increase in the cropland fraction and expanded the land suitable for crops. The grids in which the cropland fraction increased accounted for 32.16% of the total grids. During the 1850–1911, 1911–1949, and 1949–1985 periods, grids that contained cropland fractions increased because of polder construction, and these areas were distributed mainly in the central area and gradually developed from north to south, covering 6.69%, 4.92%, and 6.12%, respectively. Second, reclamation in the mountains resulted in a less than 10% increase in the cropland fraction, which was distributed mainly in the periphery of the area, and constituted 40.14% of the total grids. Third, the grids in which the cropland fraction remained nearly invariable were located in modern Dongting Lake, accounting for 26.02%. Fourth, the grids in which the cropland fraction decreased due to floods occupied 1.69% of the total grids.

(4) Changes in the land suitability for crops impacted the spatially explicit reconstruction. In the DTP, the numbers of grids unsuitable for crops were 78, 46, and 28 in approximately 1850, 1911, and 1949 with a spatial resolution of 5′ × 5′, which constituted 19.21%, 11.33%, and 6.90% of the total grids, respectively. By comparing the HYDE 3.2 and this study, the difference in cropland cover change under changing land suitability for crops was determined and understood. In the land unsuitable for crops, the proportions of grids allocated as cropland by HYDE 3.2 were 93.59%, 89.13%, and 82.14% of the total grids unsuitable for crops, respectively. This meant that the reliability of these grids was uncertainty when a spatially explicit reconstruction of the cropland change was carried out in this area. As the study period moved closer to modern time (1980s), smaller differences were observed between HYDE and this study in the land suitable for crops.

Funding information This work was supported by grants from the National Key R&D Program of China (No. 2017YFA0603304).

References

Auerbach LW, Goodbred SL Jr, Mondal DR, Wilson CA, Ahmed KR, Roy K, Steckler MS, Small C, Gilligan JM, Ackerly BA (2015) Flood risk of natural and embanked landscapes on the Ganges-Brahmaputra tidal delta plain. Nat Clim Chang 5:153–157. https://doi.org/10.1038/nclimate2472

Bakker MM, Govers G, Kosmas C, Vanacker V, Van Oost K, Rounsevell M (2005) Soil erosion as a driver of land-use change. Agric Ecosyst Environ 105:467–481. https://doi.org/10.1016/j.agee.2004.07.009

Bao J, Gao S, Ge J (2019) Dynamic land use and its policy in response to environmental and social-economic changes in China: a case study of the Jiangsu coast (1750–2015). Land Use Policy 82:169–180. https://doi.org/10.1016/j.landusepol.2018.12.008

Bayer AD, Lindeskog M, Pugh TA, Anthoni PM, Fuchs R, Arneth A (2017) Uncertainties in the land-use flux resulting from land-use change reconstructions and gross land transitions. Earth Syst Dynam 8:91–111. https://doi.org/10.5194/esd-8-91-2017

Brinson MM, Malvárez AI (2002) Temperate freshwater wetlands: types, status, and threats. Environ Conserv 29:115–133. https://doi.org/10.1017/S0376892902000085

Compilation Office of Water Resources of Hunan Province (1985) The gazetteer of water conservancy of Dongting Lake district. Water Resources of Hunan Province, Changsha

Davidson NC (2014) How much wetland has the world lost? Long-term and recent trends in global wetland area. Mar Freshw Res 65:934–941. https://doi.org/10.1071/MF14173

Department of Land and Resources of Hunan Province (2011) The historical atlas of Dongting Lake. Hunan Map Publishing House, Changsha

Department of Water Resources of Hunan Province (1987) The atlas of polder in Dongting Lake district in Hunan Province. Hunan Map Publishing House, Changsha

Department of Water Resources of Hunan Province (1989) The gazetteer of water conservancy of Dongting Lake. Water Resources of Hunan Province, Changsha

Ellis EC, Kaplan JO, Fuller DQ, Vavrus S, Goldewijk K, Verburg PH (2013) Used planet: a global history. Proc Natl Acad Sci USA 110: 7978–7985. https://doi.org/10.1073/pnas.1217241110

Erb K, Luyssaert S, Meyfroidt P, Pongratz J, Don A, Kloster S, Kuemmerle T, Fetzel T, Fuchs R, Herold M, Haberl H (2017) Land management: data availability and process understanding for global change studies. Global Chang Boil 23:512–533. https://doi.org/10.1111/gcb.13443

Gaillard MJ, Morrison K, Madella M, Whitehouse N (2018) Past land-use and land-cover change: the challenge of quantification at the sub-continental to global scales. Past Glob Change Magazine 26:3. https://doi.org/10.22498/pages.26.1.3

Garcia-Acevedo MR (2001) The confluence of water, patterns of settlement, and construction of the border in the Imperial and Mexicali valleys 1900–1999. In: Blatter J, Ingram HM (eds) Reflections on water: new approaches to transboundary conflicts and cooperation. MIT Press, Cambridge

Gedan KB, Silliman BR, Bertness MD (2009) Centuries of human-driven change in salt marsh ecosystems. Annu Rev Mar Sci 1:117–141. https://doi.org/10.1146/annurev.marine.010908.163930

Goldewijk KK (2001) Estimating global land use change over the past 300 years: the HYDE Database. Global Biogeochem Cy 15:417–433. https://doi.org/10.1029/1999GB001232

Goldewijk KK, Beusen A, van Drecht G, de Vos M (2011) The HYDE 3.1 spatially explicit database of human-induced global land-use change over the past 12,000 years. Global Ecol Biogeogr 20:73–86. https://doi.org/10.1111/j.1466-8238.2010.00587.x

Goldewijk KK, Beusen A, Doelman J, Stehfest E (2017) Anthropogenic land use estimates for the Holocene–HYDE 3.2. Earth Syst Sci Data 9:927–953. https://doi.org/10.5194/essd-9-927-2017

Gong S (1996) The agricultural geography of Hubei and Hunan in Qing dynasty. Central China Normal University Press, Wuhan

Han M (2012) Chinese historical agricultural geography. Peking University Press, Beijing

Hao Z, Zheng J, Ge Q, Wang W (2012) Winter temperature variations over the middle and lower reaches of the Yangtze River since 1736 AD. Clim Past 8:1023–1030. https://doi.org/10.5194/cp-8-1023-2012

He F, Li M, Li S (2017) Reconstruction of Lu-level cropland areas in the Northern Song Dynasty (AD976–1078). J Geogr Sci 27:606–618. https://doi.org/10.1007/s11442-017-1395-3

Hoeksema R (2007) Three stages in the history of land reclamation in the Netherlands. Irrig Drain 56(S1):S113–S126. https://doi.org/10.1002/ird.340

Kaplan JO, Krumhardt KM, Zimmermann N (2009) The prehistoric and preindustrial deforestation of Europe. Quat Sci Rev 28:3016–3034. https://doi.org/10.1016/j.quascirev.2009.09.028

Kaplan JO, Krumhardt KM, Ellis EC, Ruddiman WF, Lemmen C, Goldewijk KK (2011) Holocene carbon emissions as a result of anthropogenic land cover change. Holocene 21:775–791. https://doi.org/10.1177/0959683610386983

Li Y (2014) The development history of evolution, brief, and governance in Dongting Lake. Hunan University Press, Changsha

Li S, He F, Zhang X (2016) A spatially explicit reconstruction of cropland cover in China from 1661 to 1996. Reg Environ Chang 16:417–428. https://doi.org/10.1007/s10113-014-0751-4

Li M, He F, Yang F, Li S (2018) Reconstructing provincial cropland area in eastern China during the early Yuan Dynasty (AD1271–1294). J Geogr Sci 28:1994–2006. https://doi.org/10.1007/s11442-018-1576-8

Lu X (2016) The man-land relationship and regional society in the middle reach of Yangtze River. Xiamen University Press, Xiamen

Marks RB (2011) China: Its environment and history. Rowman & Littlefield Publishers, Lanham

Martín-Antón M, Negro V, del Campo J, López-Gutiérrez J, Esteban M (2016) Review of coastal land reclamation situation in the world. J Coast Res 75:667–671. https://doi.org/10.2112/SI75-133.1

Mei L, Zhang G, Yan C (1995) The history of the development in the plain of Hubei and Hunan. Jiangxi Education Publishing House, Nanchang

Nguyen HH, Dargusch P, Moss P, Tran DB (2016) A review of the drivers of 200 years of wetland degradation in the Mekong Delta of Vietnam. Reg Environ Chang 16:2303–2315. https://doi.org/10.1007/s10113-016-0941-3

Ramankutty N, Foley JA (1999) Estimating historical changes in global land cover: croplands from 1700 to 1992. Glob Biogeochem Cycles 13:997–1027. https://doi.org/10.1029/1999gb900046

Segeren WA (1983) Introduction to Polders of the World. Water Int 8:51–54. https://doi.org/10.1080/02508068308686006

Verhoeven JT, Setter TL (2010) Agricultural use of wetlands: opportunities and limitations. Ann Bot 105:155–163. https://doi.org/10.1093/aob/mcp172

Wang J, Gao M, Guo H, Chen E (2016) Spatiotemporal distribution and historical evolution of polders in the Dongting Lake area, China. J Geogr Sci 26:1561–1578. https://doi.org/10.1007/s11442-016-1344-6

Waz A, Creed IF (2017) Automated techniques to identify lost and restorable wetlands in the Prairie Pothole Region. Wetlands 37:1079–1091. https://doi.org/10.1007/s13157-017-0942-0

Wei X, Ye Y, Zhang Q, Fang X (2015) Methods for cropland reconstruction based on gazetteers in the Qing dynasty (1644–1911): a case study in Zhili Province, China. Appl Geogr 65:82–92. https://doi.org/10.1016/j.apgeog.2015.11.002

Wei X, Ye Y, Zhang Q, Fang X (2016) Reconstruction of cropland change over the past 300 years in the Jing-Jin-Ji area, China. Reg Environ Chang 16:2097–2109. https://doi.org/10.1007/s10113-016-0933-3

Wei X, Ye Y, Zhang Q, Li B, Wei Z (2019) Reconstruction of cropland change in North China Plain Area over the past 300 years. Glob Planet Chang 176:60–70. https://doi.org/10.1016/j.gloplacha.2019.01.010

Wu G, Hao Z, Zheng J (2010) Reconstruction and analysis of seasonal precipitation in Nanjing since 1736. Sci Geogr Sin 30:936–942. https://doi.org/10.13249/j.cnki.sgs.2010.06.005

Yang X, Jin X, Du X, Xiang X, Han J, Shan W, Fan Y, Zhou Y (2016) Multi-agent model-based historical cropland spatial pattern reconstruction for 1661–1952, Shandong Province, China. Glob Planet Chang 143:175–188. https://doi.org/10.1016/j.gloplacha.2016.06.010

Ye Y, Fang X, Ren Y, Zhang X, Chen L (2009) Cropland cover change in Northeast China during the past 300 years. Sci China Earth Sci 52: 1172–1182. https://doi.org/10.1007/s11430-009-0118-8

Ye Y, Wei X, Li F, Fang X (2015) Reconstruction of cropland cover changes in the Shandong Province over the past 300 years. Sci Rep 5:13642. https://doi.org/10.1038/srep13642

Yuan C, Ye Y, Tang C, Fang X (2017) Accuracy Comparison of Gridded Historical Cultivated Land Data in Jiangsu and Anhui Provinces. Chin Geogr Sci 27:273–285. https://doi.org/10.1007/s11769-017-0862-1

Zhang X, Luo Z, Wu X, Chen X (1999) The economy of Hunan over the past 50 years. Hunan People's Publishing House, Changsha

Zou Y, Zhang X, Wang S (2013) The physical geography in Chinese history. Science Press, Beijing